

Integral cross section measurement of the $^{12}\text{C}(\text{n,p})^{12}\text{B}$ reaction

*P. Žugec*¹⁶, *N. Colonna*², *D. Bosnar*¹, *A. Ventura*³, *A. Mengoni*⁴, *S. Altstadt*⁵, *J. Andrzejewski*⁶, *L. Audouin*⁷, *M. Barbagallo*², *V. Bécaries*⁸, *F. Bečvář*⁹, *F. Belloni*¹⁰, *E. Berthoumieux*¹¹, *J. Billowes*¹², *V. Boccone*¹³, *M. Brugger*¹³, *M. Calviani*¹³, *F. Calviño*¹⁴, *D. Cano-Ott*⁸, *C. Carrapiço*¹⁵, *F. Cerutti*¹³, *E. Chiaveri*¹³, *M. Chin*¹³, *G. Cortés*¹⁴, *M.A. Cortés-Giraldo*¹⁶, *L. Cosentino*¹⁷, *M. Diakaki*¹⁸, *C. Domingo-Pardo*¹⁹, *R. Dressler*²⁰, *I. Duran*²¹, *C. Eleftheriadis*²², *A. Ferrari*¹³, *P. Finocchiaro*¹⁷, *K. Fraival*¹¹, *S. Ganesan*²³, *A.R. García*⁸, *G. Giubrone*¹⁹, *M.B. Gómez-Hornillos*¹⁴, *I.F. Gonçalves*¹⁵, *E. González-Romero*⁸, *E. Griesmayer*²⁴, *C. Guerrero*¹³, *F. Gunsing*¹¹, *P. Gurusamy*²³, *S. Heinitz*²⁰, *D.G. Jenkins*²⁵, *E. Jericha*²⁴, *F. Käppeler*²⁶, *D. Karadimos*¹⁸, *N. Kivel*²⁰, *M. Kokkoris*¹⁸, *M. Krtička*⁹, *J. Kroll*⁹, *C. Langer*⁵, *C. Lederer*⁵, *H. Leeb*²⁴, *L.S. Leong*⁷, *S. Lo Meo*⁴, *R. Losito*¹³, *A. Manouosos*²², *J. Marganiec*⁶, *T. Martínez*⁸, *C. Massimi*²⁷, *P. Mastinu*²⁸, *M. Mastromarco*², *E. Mendoza*⁸, *P.M. Milazzo*²⁹, *F. Mingrone*²⁷, *M. Mirea*³⁰, *W. Mondalaers*¹⁰, *A. Musumarra*³¹, *C. Paradela*¹⁰, *A. Pavlik*³², *J. Perkowski*⁶, *A. Plompen*¹⁰, *J. Praena*¹⁶, *J. Quesada*¹⁶, *T. Rauscher*^{33,34}, *R. Reifarth*⁵, *A. Riego*¹⁴, *F. Roman*¹³, *C. Rubbia*¹³, *R. Sarmiento*¹⁵, *A. Saxena*²³, *P. Schillebeeckx*¹⁰, *S. Schmidt*⁵, *D. Schumann*²⁰, *G. Tagliente*², *J.L. Tain*¹⁹, *D. Tarrío*²¹, *L. Tassan-Got*⁷, *A. Tsinganis*¹³, *S. Valenta*⁹, *G. Vannini*²⁷, *V. Variale*², *P. Vaz*¹⁵, *R. Versaci*¹³, *M.J. Vermeulen*²⁵, *V. Vlachoudis*¹³, *R. Vlastou*¹⁸, *A. Wallner*^{35,32}, *T. Ware*¹², *M. Weigand*⁵, *C. Weiss*¹³, *T. Wright*¹²

¹Department of Physics, Faculty of Science, University of Zagreb, Croatia;

²Istituto Nazionale di Fisica Nucleare, Sezione di Bari, Italy;

³Istituto Nazionale di Fisica Nucleare, Sezione di Bologna, Italy;

⁴ENEA, Bologna, Italy;

⁵Johann-Wolfgang-Goethe Universität, Frankfurt, Germany;

⁶Uniwersytet Łódzki, Lodz, Poland;

⁷Centre National de la Recherche Scientifique/IN2P3 - IPN, Orsay, France;

⁸Centro de Investigaciones Energéticas Medioambientales y Tecnológicas (CIEMAT), Madrid, Spain;

⁹Charles University, Prague, Czech Republic;

¹⁰European Commission JRC, Institute for Reference Materials and Measurements, Retieseweg 111, B-2440 Geel, Belgium;

¹¹CEA/Saclay - IRFU, Gif-sur-Yvette, France;

¹²University of Manchester, Oxford Road, Manchester, UK;

¹³CERN, Geneva, Switzerland;

¹⁴Universitat Politècnica de Catalunya, Barcelona, Spain;

¹⁵C2TN-Instituto Superior Técnico, Universidade de Lisboa, Portugal;

¹⁶Universidad de Sevilla, Spain;

¹⁷INFN - Laboratori Nazionali del Sud, Catania, Italy;

¹⁸National Technical University of Athens (NTUA), Greece;

¹⁹Instituto de Física Corpuscular, CSIC-Universidad de Valencia, Spain;

²⁰Paul Scherrer Institut, 5232 Villigen PSI, Switzerland;

²¹Universidade de Santiago de Compostela, Spain;

²²Aristotle University of Thessaloniki, Thessaloniki, Greece;

²³Bhabha Atomic Research Centre (BARC), Mumbai, India;

²⁴Atominstytut der Österreichischen Universitäten, Technische Universität Wien, Austria;

²⁵University of York, Heslington, York, UK;

²⁶Karlsruhe Institute of Technology (KIT), Institut für Kernphysik, Karlsruhe, Germany;

²⁷Dipartimento di Fisica, Università di Bologna, and Sezione INFN di Bologna, Italy;

²⁸Istituto Nazionale di Fisica Nucleare, Laboratori Nazionali di Legnaro, Italy;

²⁹Istituto Nazionale di Fisica Nucleare, Sezione di Trieste, Italy;

³⁰Horia Hulubei National Institute of Physics and Nuclear Engineering - IFIN HH, Bucharest - Magurele,

Romania;

³¹Dipartimento di Fisica e Astronomia DFA, Università di Catania and INFN-Laboratori Nazionali del Sud, Catania, Italy;

³²University of Vienna, Faculty of Physics, Austria;

³³Centre for Astrophysics Research, School of Physics, Astronomy and Mathematics, University of Hertfordshire, Hatfield, United Kingdom;

³⁴Department of Physics, University of Basel, Basel, Switzerland;

³⁵Research School of Physics and Engineering, Australian National University, ACT 0200, Australia

Abstract

The integral cross section of the $^{12}\text{C}(n, p)^{12}\text{B}$ reaction was measured at the neutron time of flight facility n_TOF at CERN, from the reaction threshold at 13.6 MeV up to 10 GeV, by means of the combined activation and a time-of-flight technique. The integral result is expressed as the number of ^{12}B nuclei produced per single pulse of the neutron beam. A simple integral expression is given for calculating the number of produced ^{12}B nuclei from any given evaluated cross section and/or model prediction.

1. Introduction

Nuclear medicine, radiological protection, the design of the structural materials at neutron production facilities and the design of detectors used for fundamental nuclear physics experiments are some of the fields where data on the neutron induced $^{12}\text{C}(n, p)^{12}\text{B}$ reaction play an important role. In nuclear medicine – in particular in hadrontherapy – and in radiological protection this reaction must be taken into account when estimating the dose received by biological tissues, which is built up both by protons, as the primary reaction products, and by the highly energetic electrons from a subsequent β -decay of ^{12}B ($Q = 13.37$ MeV). At neutron production facilities where the neutron flux extends above the reaction threshold of 13.6 MeV, the emission of protons from the $^{12}\text{C}(n, p)^{12}\text{B}$ reaction leads to the production of hydrogen within the steel alloys, increasing the risk of embrittlement. In fundamental nuclear physics experiments carbon is often used both as the detector housing material and as the main chemical constituent of the active material, e.g. C_6D_6 (historically, C_6F_6 detectors) due to its extremely low neutron capture cross section providing a very low intrinsic sensitivity to scattered neutrons. However, in the presence of high energy neutrons, the $^{12}\text{C}(n, p)^{12}\text{B}$ reaction may give rise to an additional component in the neutron background and even compromise the experimental estimation of the neutron background by means of neutron irradiation of the carbon sample [1].

Despite these considerations, the experimental data on the $^{12}\text{C}(n, p)^{12}\text{B}$ reaction are very scarce and largely discrepant from each other [2, 3, 4, 5, 6, 7], as clearly shown in Fig. 1. This lack of data is also reflected in the inability of the different models to consistently predict the cross section, and thus the ^{12}B production rate of this reaction. For illustration, Fig. 1 also shows the cross sections extracted from several different models available in GEANT4 [8] – the HP (High Precision) package, Binary cascade, Bertini cascade, INCL++/ABLA model (INCL intranuclear cascade coupled to the ABLA deexcitation model) and QGS (Quark-Gluon-String) model [9]. It should be noted that HP package adopts the cross section directly from the ENDF/B-VII.1 database [10], while the other cross sections are the results of the model calculations.

The integral cross section of the $^{12}\text{C}(n, p)^{12}\text{B}$ reaction was measured at the neutron time of flight facility n_TOF at CERN, from the reaction threshold at 13.6 MeV up to 10 GeV. Although this integral value cannot be directly compared to past experimental data – all energy dependent and limited to a

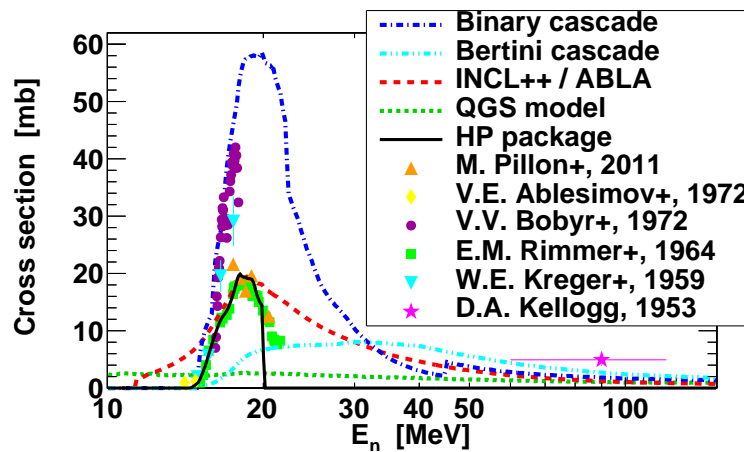


Fig. 1: Cross sections of $^{12}\text{C}(n,p)^{12}\text{B}$ reaction from different GEANT4 models, compared to the available experimental data.

reduced energy range – it may be used as a validation benchmark for different cross section evaluations and/or model calculations.

2. Experimental setup

At the n_TOF facility the neutron beam is produced by exposing the massive Pb spallation target to a pulsed proton beam from the CERN Proton Synchrotron. The proton beam is characterized by an energy of 20 GeV, an average of 7×10^{12} protons per pulse, 7 ns width, minimal repetition period of 1.2 s and a typical frequency of 0.4 Hz. The neutron beam (with ~ 300 neutrons produced per single proton) is moderated passing through the spallation target, through 1 cm of demineralized water from a cooling system and additional 4 cm of borated water. After moderation, the neutron flux spans an energy range from thermal (~ 10 meV) up to 10 GeV. Passing through an evacuated beam line towards the Experimental Area 1 at 185 m distance from the spallation target, charged particles are removed from the beam by a 1.5 T sweeping magnet and is shaped by two collimators. A more detailed description of the n_TOF facility may be found in Ref. [11]. We refer the reader to Ref. [12] for an in-depth description of the neutron flux measurements at n_TOF.

The integral cross section measurement of the $^{12}\text{C}(n,p)^{12}\text{B}$ reaction was performed using a natural carbon sample of 7.13 g mass, 2 cm diameter, 1 cm thickness and a chemical purity of 99.95%, which was confirmed at the Paul Scherrer Institute. The experiment relies on the detection of β -rays, with an average energy of 6.35 MeV, from the decay of ^{12}B produced by the $^{12}\text{C}(n,p)^{12}\text{B}$ reaction. Two deuterated benzene (C_6D_6) liquid scintillation detectors were used for the detection of these β -rays. One is the modified version of the Bicron detector, while the other one (denoted as FZK) is a custom built detector from Forschungszentrum Karlsruhe, Germany. These detectors, commonly used at n_TOF for neutron capture measurements, have been optimized with the specific purpose of achieving a very low sensitivity to scattered neutrons [13]. Further details on the methodology of the experiment may be found in Refs. [14, 15].

The ^{12}B half-life of 20.2 ms is highly beneficial to the experiment, since the data acquisition window of 96 ms is sufficient to cover a significant portion of the ^{12}B exponential decay distribution. A description of a high-performance digital data acquisition system at n_TOF – based on 8-bit flash analog-to-digital converter units (FADC) with 48 MB memory buffer, operating at a typical sampling rate of 500 MHz – may be found in Ref. [16].

3. Data analysis

There are several sources of background affecting the measurement, all of which have been clearly identified. The first background component, related to the scattering of in-beam γ -rays off the ^{nat}C sample, was measured with a Pb sample and was found completely negligible. The background caused by the neutron beam crossing the experimental area was measured by irradiating the overall experimental setup without the sample in place. The ambient background, caused by the natural and induced radioactivity, was measured by turning off the neutron beam. All experimentally accessible background components were properly normalized and subtracted from the measurements with the ^{nat}C sample.

Finally, the neutron background, which is caused by neutron scattering off the sample, has been determined by means of recently developed high-precision GEANT4 simulations [1]. The simulated results have been found to be highly reliable, based on the comparison with experimental data obtained with a ^{nat}C sample. However, it was shown in Ref. [1] that the simulated neutron background which is composed mostly of the capture γ -rays, can be reliably described only by applying the Pulse Height Weighting Technique (PHWT) [17]. This procedure is commonly used in the analysis of neutron capture data obtained by detectors with a low γ -ray detection efficiency (the details on the PHWT applied at n_TOF may be found in Ref. [18]). In short, the lack of proper correlations between the simulated capture γ -rays modifies their energy distribution (relative to the experimental one), thus affecting the average detection efficiency for capture events. Applying the PHWT removes the effect of these correlations, the only condition being that the energy conservation is respected in the generation of capture γ -rays.

The PHWT is performed by assigning to each detected count a weighting factor $W(E)$, dependent on the energy E deposited in the detector. The weighting of the experimental counts $C_{\text{exp}}(t)$, expressed as a function of the decay time t , may be decomposed as:

$$W(E) \otimes C_{\text{exp}}(t) = W(E) \otimes C_{\gamma}(t) + \langle W \rangle \times C_{\beta}(t) \quad (1)$$

The application of the weighting factors is symbolically denoted by \otimes . $C_{\gamma}(t)$ is the neutron background, mostly composed of the capture γ -rays from the experimental area. $C_{\beta}(t)$ is the time distribution of detected β -rays from a decay of ^{12}B . Owing to the fact that there are no correlations between β -rays, the application of the PHWT to the corresponding spectrum $C_{\beta}(t)$ is reduced to a simple multiplication by the average weighting factor $\langle W \rangle$:

$$\langle W \rangle = \frac{\int_{200\text{keV}}^{13.37\text{MeV}} S_{\beta}(E)W(E)dE}{\int_{200\text{keV}}^{13.37\text{MeV}} S_{\beta}(E)dE} \quad (2)$$

which is directly determined by the energy spectrum $S_{\beta}(E)$ of the detected β -rays. The lower integration bound from Eq. (2) is equal to the threshold set during the data analysis. The upper bound is given by the Q -value of the ^{12}B decay. The energy spectrum $S_{\beta}(E)$, which is easily determined from simulations, allows to invert Eq. (1) and to obtain the unweighted experimental spectrum of detected β -rays:

$$C_{\beta}(t) = \frac{W(E) \otimes C_{\text{exp}}(t) - W(E) \otimes C_{\gamma}(t)}{\langle W \rangle} \quad (3)$$

The remaining spectrum corresponds to the time distribution of the ^{12}B decay:

$$C_{\beta}(t) = \frac{\varepsilon_{\beta} N_{^{12}\text{B}}}{\tau} e^{-t/\tau} \quad (4)$$

with $\tau = 29.14$ ms as the lifetime of ^{12}B and ε_{β} as the total detection efficiency of C_6D_6 detectors, de-

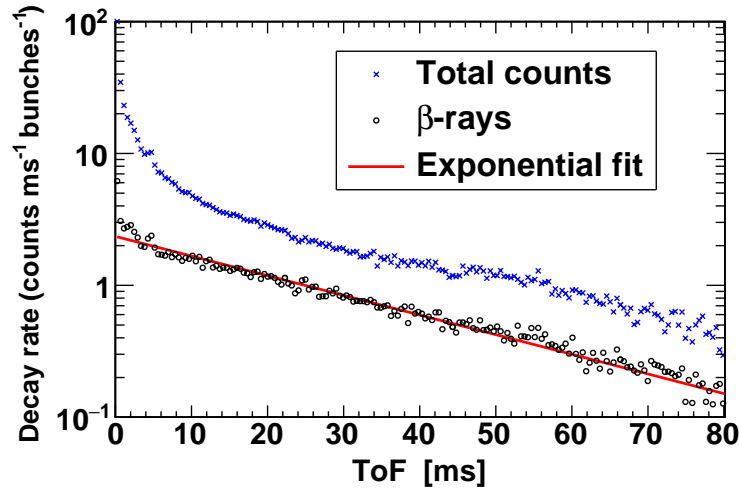


Fig. 2: Time distribution of ^{12}B decays, measured by two C_6D_6 detectors. The spectra show the total counts C from two detectors summed together, and normalized by the sum of their respective detection efficiencies ε : $(C_{\text{Bicron}} + C_{\text{FZK}})/(\varepsilon_{\text{Bicron}} + \varepsilon_{\text{FZK}})$.

terminated from the simulations (4.3% for Bicron, 6.8% for FZK). The spectra before and after the background subtraction, obtained by combining the data from both detectors, are shown in Fig. 2. The number $N_{^{12}\text{B}}$ of ^{12}B nuclei produced per single neutron bunch was found by fitting (up to 80 ms) the spectrum $C_{\beta}(t)$ to the exponential from Eq. (4), with $N_{^{12}\text{B}}$ as the only free parameter. The combination of the highly consistent results from the two detectors – $N_{^{12}\text{B}}^{(\text{Bicron})} = 68.03 \pm 0.66$ and $N_{^{12}\text{B}}^{(\text{FZK})} = 68.74 \pm 0.44$ – yields the final value of $N_{^{12}\text{B}} = 68.5 \pm 0.4_{\text{stat}} \pm 4.8_{\text{sys}}$. A systematic uncertainty of 2% was assigned to the contribution of β -rays produced outside the $^{\text{nat}}\text{C}$ sample. An additional 3% uncertainty was introduced due to the highly uncertain (n, p) , (n, d) and (n, np) reactions on ^{13}C present in natural carbon, leading to the production of both ^{12}B and ^{13}B , with the decay properties of ^{13}B being very similar to those of ^{12}B .

4. Integral cross section

The number of ^{12}B nuclei produced per neutron bunch may be brought into connection with the underlying cross section $\sigma(E_n)$ of the $^{12}\text{C}(n, p)^{12}\text{B}$ reaction:

$$N_{^{12}\text{B}} = \int_{13.6\text{MeV}}^{10\text{GeV}} \frac{1 - e^{-n\sigma_{\text{tot}}(E_n)}}{\sigma_{\text{tot}}(E_n)} \eta(E_n) \phi(E_n) \sigma(E_n) dE_n \quad (5)$$

where the lower integration limit corresponds to the reaction threshold, while the upper one corresponds to the maximal energy of the n_TOF neutron beam. The first term represents the self-shielding factor, determined by the areal density n of the $^{\text{nat}}\text{C}$ sample ($n = 0.114$ atoms/barn) and the total cross section $\sigma_{\text{tot}}(E_n)$, available from various evaluated libraries, such as ENDF/B-VII.1 [10]. Multiplied by $\sigma(E_n)$, it determines the first chance yield of the $^{12}\text{C}(n, p)^{12}\text{B}$ reaction, not taking into account the multiple scattering effect. This is accounted for separately, by the factor $\eta(E_n)$. The energy dependence of the multiple scattering factor throughout the entire energy range from the reaction threshold up to 10 GeV was obtained by simulating the neutron irradiation of the $^{\text{nat}}\text{C}$ sample, using different GEANT4 models for the ^{12}B production. It is to be noted that the elastic cross section is independent of the inelastic scattering models. Starting from widely different cross sections for the $^{12}\text{C}(n, p)^{12}\text{B}$ reaction (see

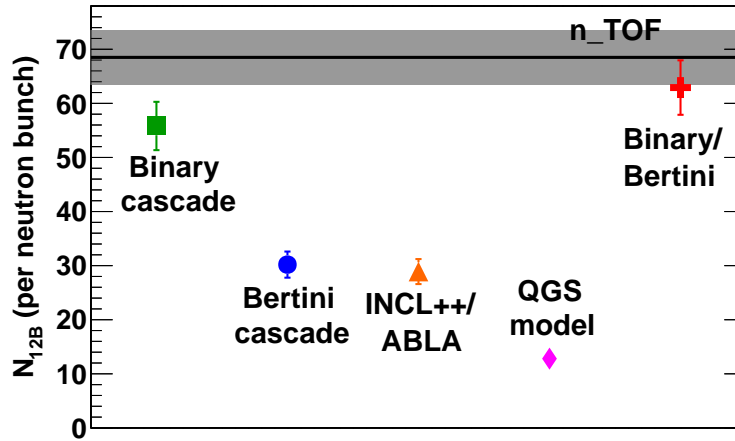


Fig. 3: Number of produced ^{12}B nuclei per single neutron pulse of the n_TOF beam, as predicted by different GEANT4 models. The values have been calculated by means of Eq. (5) and are compared to the experimental value (full line with the associated uncertainty range).

Fig. 1), all models yield very consistent multiple scattering corrections, confirming the reliability of the result. Finally, the neutron flux $\phi(E_n)$ from Eq. (5) was measured up to 1 GeV by the Parallel Plate Avalanche Counters (PPAC [19]), relying on the $^{235}\text{U}(n, f)$ reaction. Further details on the neutron flux measurements at n_TOF may be found in Ref. [12]. The neutron flux evaluation was extended above 1 GeV, based on the results from the dedicated GEANT4 simulations, normalized to the experimental data below 1 GeV. The overall energy dependent term multiplying the cross section $\sigma(E_n)$ from Eq. (5) may be treated as a unique weighting function $w(E_n)$, which was fitted to the fifth degree polynomial:

$$\log_{10} \frac{w(E_n)}{w_0} = \sum_{m=0}^5 a_m \left(\log_{10} \frac{E_n}{E_0} \right)^m \quad (6)$$

with $E_0 = 1$ MeV and $w_0 = 1$ MeV $^{-1}$ mb $^{-1}$. The fit yields the following parameters: $a_0 = 12.9676$, $a_1 = -33.9199$, $a_2 = 32.3332$, $a_3 = -15.0657$, $a_4 = 3.36573$ and $a_5 = -0.291966$. The weighting function has been assigned 8% systematic uncertainty, coming from the uncertainties in each of its components – the neutron flux, self shielding and the multiple scattering factor.

With the weighting function $w(E_n)$ uniquely identified, any pointwise cross section for the $^{12}\text{C}(n, p)^{12}\text{B}$ reaction that extends over the full energy range from the reaction threshold up to 10 GeV, may be used to calculate the associated number of the ^{12}B nuclei produced per single neutron pulse of the n_TOF beam. In this way any cross section calculation or evaluation may be benchmarked against the experimental n_TOF result. This has been done for the different GEANT4 models, adopting the cross sections from Fig. 1. The results are shown in Fig. 3. Alongside results from all models extending all the way up to 10 GeV, the result from a combined Binary and Bertini cascade is also shown. The combination of Binary cascade up to 30 MeV and Bertini cascade above 30 MeV maximizes the cross section for $^{12}\text{C}(n, p)^{12}\text{B}$ reaction, yielding the integral result closest to the experimental one.

The secondary quantities such as the value analogous to the resonance integral I_{12B} :

$$I_{12B} = \int_{13.6\text{MeV}}^{10\text{GeV}} \frac{\sigma(E_n)}{E_n} dE_n \approx \frac{N_{12B}}{\kappa} \quad (7)$$

may also be estimated. The conversion factor κ between the number of produced ^{12}B nuclei (the true observable) and the convenient quantity $I_{12\text{B}}$ was determined to be $\kappa = 1.85 \pm 0.1 \text{ mb}^{-1}$, yielding the value $I_{12\text{B}} = 37 \pm 3 \text{ mb}$.

5. Conclusions

The integral cross section of the $^{12}\text{C}(n,p)^{12}\text{B}$ reaction was measured at the neutron time of flight facility n_TOF at CERN. A high-purity $^{\text{nat}}\text{C}$ sample was exposed to an intense, white, pulsed neutron beam, covering the energy range from below the reaction threshold at 13.6 MeV, up to 10 GeV. The measurement was performed by detecting the β -rays from the decay of the produced ^{12}B nuclei. Two liquid scintillation C_6D_6 detectors were used, which are commonly employed at n_TOF for the neutron capture measurements, due to their very low intrinsic sensitivity to the scattered neutrons. All sources of background were clearly identified – either by the dedicated measurements or simulations – and subtracted from the measurements with a high-purity $^{\text{nat}}\text{C}$ sample. The remaining time distribution of β -decays was fitted to an exponential form with the lifetime of ^{12}B , thus obtaining the number of ^{12}B nuclei produced per neutron pulse: $N_{12\text{B}} = 68.5 \pm 0.4_{\text{stat}} \pm 4.8_{\text{sys}}$. This observable was related to the cross section of the $^{12}\text{C}(n,p)^{12}\text{B}$ reaction, by means of a properly determined weighting function, which has been used to calculate the expected number of ^{12}B nuclei produced per single pulse of the n_TOF beam.

Acknowledgements

This research was funded by the European Atomic Energy Community's (Euratom) Seventh Framework Programme FP7/2007-2011 under the Project CHANDA (Grant No. 605203) and by the Croatian Science Foundation under Project No. 1680. GEANT4 simulations have been run at the Laboratory for Advanced Computing, Faculty of Science, University of Zagreb.

References

- [1] P. Žugec, N. Colonna, D. Bosnar *et al.*, Nucl. Instr. and Meth. A **760**, 57 (2014).
- [2] M. Pillon, M. Angelone, A. Krása *et al.*, Nucl. Instr. and Meth. A **640**, 185 (2011).
- [3] V. E. Ablesimov, E. K. Bonjushkin and A. P. Morosov, in *Neutron Physics Conf., Kiev 1971*, Vol.1, p.173 (1971).
- [4] W. E. Kreger and B. D. Kern, Phys. Rev. **113**, 890 (1959).
- [5] E. M. Rimmer and P. S. Fisher, Nucl. Phys. A **108**, 567 (1968).
- [6] V. V. Bobyr, G. I. Primenko, K. K. Revyuk *et al.*, Izv. Akad. Nauk SSSR, Ser. Fiz. **36**, 2621 (1972) (in Russian).
- [7] D. A. Kellogg, Phys. Rev. **90**, 224 (1953).
- [8] S. Agostinelli, J. Allison, K. Amako *et al.*, Nucl. Instr. and Meth. A **506**, 250 (2003).
- [9] GEANT4 *Physics Reference Manual*, <http://geant4.cern.ch/>.
- [10] M. B. Chadwick, M. Herman, P. Obložinský *et al.*, Nucl. Data Sheets **112**, 2887 (2011).
- [11] C. Guerrero, A. Tsinganis, E. Berthoumieux *et al.*, Eur. Phys. J. A **49**, 27 (2013).
- [12] M. Barbagallo, C. Guerrero, A. Tsinganis *et al.*, Eur. Phys. J. A **49**, 156 (2013).
- [13] R. Plag, M. Heil, F. Käppeler *et al.*, Nucl. Instr. and Meth. A **496**, 425 (2003).
- [14] P. Žugec, N. Colonna, D. Bosnar *et al.*, Phys. Rev. C **90**, 021601(R) (2014).
- [15] P. Žugec, N. Colonna, D. Bosnar *et al.*, *Measurement of the $^{12}\text{C}(n,p)^{12}\text{B}$ integral cross section up to 10 GeV*, submitted to Physical Review C.
- [16] U. Abbondanno, G. Aerts, F. Álvarez *et al.*, Nucl. Instr. and Meth. A **538**, 692 (2005).
- [17] R. L. Macklin, and J. H. Gibbons, Phys. Rev. **159**, 1007 (1967).
- [18] U. Abbondanno, G. Aerts, H. Alvarez *et al.*, Nucl. Instr. and Meth. A **521**, 454 (2004).
- [19] C. Paradela, L. Tassan-Got, L. Audouin *et al.*, Phys. Rev. C **82**, 034601 (2010).